

## Article

# Tracking the Dynamics of *Spartina alterniflora* with WorldView-2/3 and Sentinel-1/2 Imagery in Zhangjiang Estuary, China

Di Dong<sup>1,2,3</sup>, Huamei Huang<sup>1,3,\*</sup> and Qing Gao<sup>1,3</sup>

<sup>1</sup> South China Sea Institute of Planning and Environment Research, State Oceanic Administration, Guangzhou 510300, China; dongdide90@163.com (D.D.); gaoqing182020@163.com (Q.G.)

<sup>2</sup> Key Laboratory of Marine Environmental Survey Technology and Application, Ministry of Natural Resources, Guangzhou 510300, China

<sup>3</sup> Technology Innovation Center for South China Sea Remote Sensing, Surveying and Mapping Collaborative Application, Ministry of Natural Resources, Guangzhou 510300, China

\* Correspondence: scsmeei@163.com

**Abstract:** The invasion of *Spartina alterniflora* (*S. alterniflora*) has posed serious threats to the sustainability, quality and biodiversity of coastal wetlands. To safeguard coastal ecosystems, China has enacted large-scale *S. alterniflora* removal projects, which set the goal of effectively controlling *S. alterniflora* throughout China by 2025. The accurate monitoring of *S. alterniflora* with remote sensing is urgent and requisite for the scientific eradication, control and management of this invasive plant. In this study, we combined multi-temporal WorldView-2/3 (WV-2/3) and Sentinel-1/2 imagery to monitor the *S. alterniflora* dynamics before and after the *S. alterniflora* removal projects in Zhangjiang Estuary. We put forward a new method for *S. alterniflora* detection with eight-band WV-2/3 imagery. The proposed method first used NDVI to discriminate *S. alterniflora* from water, mud flats and mangroves based on Ostu thresholding and then used the red-edge, NIR1 and NIR2 bands and support vector machine (SVM) classifier to distinguish *S. alterniflora* from algae. Due to the contamination of frequent cloud cover and tidal inundation, the long revisit time of high-resolution satellite sensors and the short-term *S. alterniflora* removal projects, we combined Sentinel-1 SAR time series and Sentinel-2 optical imagery to monitor the *S. alterniflora* removal project status in 2023. The overall accuracies of the *S. alterniflora* detection results here are above 90%. Compared with the traditional SVM method, the proposed method achieved significantly higher identification accuracy. The *S. alterniflora* area was 115.19 hm<sup>2</sup> in 2015, 152.40 hm<sup>2</sup> in 2017 and 15.29 hm<sup>2</sup> in 2023, respectively. The generated *S. alterniflora* maps clearly show the clonal growth of *S. alterniflora* in Zhangjiang Estuary from 2015 to 2017, and the large-scale *S. alterniflora* eradication project has achieved remarkable results with a removal rate of about 90% in the study area. With the continuous implementation of the “Special Action Plan for the Prevention and Control of *Spartina alterniflora* (2022–2025)” which aims to eliminate more than 90% of *S. alterniflora* in all provinces in China by 2025, the continual high-spatial resolution monitoring of *S. alterniflora* is crucial to control secondary invasion and restore coastal wetlands.

**Keywords:** *Spartina alterniflora*; remote sensing; WorldView-3; Sentinel-2; invasive species; coastal wetlands



**Citation:** Dong, D.; Huang, H.; Gao, Q. Tracking the Dynamics of *Spartina alterniflora* with WorldView-2/3 and Sentinel-1/2 Imagery in Zhangjiang Estuary, China. *Water* **2024**, *16*, 1780. <https://doi.org/10.3390/w16131780>

Academic Editors: Hans Brix, José Luis Sánchez-Lizaso and Silvia Marková

Received: 5 April 2024

Revised: 15 June 2024

Accepted: 18 June 2024

Published: 23 June 2024



**Copyright:** © 2024 by the authors. Licensee MDPI, Basel, Switzerland. This article is an open access article distributed under the terms and conditions of the Creative Commons Attribution (CC BY) license (<https://creativecommons.org/licenses/by/4.0/>).

## 1. Introduction

Salt marshes are one of the most productive systems on earth [1], providing valuable ecosystem services, such as coastline protection from storm damage and erosion, habitat for different animals, carbon storage, and water purification [2–5]. *Spartina alterniflora* (*S. alterniflora*), a perennial salt marsh grass introduced to China in 1979 for tidal reclamation and erosion mitigation [6], has rapidly spread along Chinese coasts [7–10]. Despite the

positive effects like other salt marshes [3,4,11], *S. alterniflora* has brought many ecological problems and posed serious threats to the sustainability of coastal wetlands in China [6]. *S. alterniflora* invaded tidal lands, threatened biodiversity and ecosystem stability, and disturbed the succession of native salt marsh species [12]. In 2022, five ministries in China issued the “Special Action Plan for the Prevention and Control of *Spartina Alterniflora* (2022–2025)”, which aims to effectively eliminate *S. alterniflora* with a removal rate of over 90% in all provinces by 2025 [13,14]. Accurately monitoring the expansion and removal of *S. alterniflora* is significant for the effective evaluation of the *S. alterniflora* removal projects, which supports coastal wetland management and restoration.

Compared with the traditional time-consuming and labor-intensive field survey methods, remote sensing provides an effective alternative for large-scale *S. alterniflora* monitoring [10,15–18]. Medium-resolution satellite images, such as Landsat and Sentinel-2, have been extensively applied to map *S. alterniflora* [1,15–17,19–22] with a limited capacity to identify invasive plants of small patches [23,24]. Researchers have resorted to high spatial resolution satellite imagery [23–26] and unmanned aerial vehicle (UAV) imagery [27,28] for fine-scale salt marsh classification. Liu et al. [15] used high-resolution imagery from Google Earth (GE) with three spectral bands (red, green and blue) to monitor the dynamics of *S. alterniflora* in Zhangjiang Estuary from 2003 to 2015. Zhu et al. [18] collected multi-temporal UAV RGB images and investigated the growth of *S. alterniflora* in Zhangjiang Estuary by manual screen digitalization. Windle et al. [29] gathered multi-temporal multispectral UAV images and used the supervised random forest classification method to monitor *S. alterniflora* distributions from 2019 to 2022 in Chesapeake Bay, USA. High spatial resolution satellite sensors generally have four standard bands (red, green, blue and near-infrared), whereas the launch of Worldview-2/3 (WV-2/3) makes the high spatial and spectral resolution satellite imagery available. In addition to the four standard bands, the WV-2/3 multispectral sensor provides four new multispectral bands (coastal, yellow, red edge, and near-infrared 2), which enhances remote sensing applications. Chen et al. [24] made fine-scale maps of the *S. alterniflora* in Dandou Sea using synthetic high-resolution image time series derived from the spatiotemporal fusion of WV-2 and Sentinel-2 satellite imagery. But the frequent cloud cover in coastal regions and long revisit time of high-resolution satellite sensors makes the high-resolution image time series collection still a challenge [24], which limits the use of spatiotemporal fusion methods for moderate- and high-resolution images.

Different classification methods, such as maximum likelihood [1], random forest [30,31], support vector machine (SVM) [20,25], simulated annealing algorithm [31], object-based segmentation and classification methods [15,16], as well as deep learning [32,33], have been applied to map invasive plants. Based on Landsat image time series, Tian et al. [20] proposed a pixel-based phonological feature composite method (Ppf-CM) and compared the *S. alterniflora* detection results from the SVM method and a deep learning method (Stacked AutoEncoder) in the Beibu Gulf of China. Wang et al. [34] combined the Ppf-CM method with an unsupervised multiscale segmentation method and SVM classifier to produce *S. alterniflora* maps, using Sentinel-2 imagery in Dandou Sea, Guangxi, China. Sun et al. [35] used the eXtreme Gradient Boosting algorithm to classify salt marsh species based on Landsat time series in Jiangsu, China. Zhao et al. [36] proposed a multiple attention network based on transfer learning for the semantic segmentation of *S. alterniflora* using multi-temporal Landsat images. Zhao et al. [37] put forward an intermediate domain prototype class-level learning network for *S. alterniflora* segmentation with a Landsat time series. Li et al. [38] utilized the DeepLabv3+ method to produce annual *S. alterniflora* maps in the mainland of China. Most of the machine learning methods mentioned above have been widely used for land cover classification, whereas deep learning methods demand lots of samples for training, which is tedious or even challenging due to the lack of historical high-resolution images or field survey datasets [38]. In addition, spectral confusion problems in the dynamic and complex coastal regions, such as the seasonal-dependent environmental noises (algae), degrade salt marsh classification accuracies [31].

Here, our overarching goal is to monitor the dynamics of *S. alterniflora* by combing multi-temporal WV-2/3 and Sentinel-1/2 imagery before and after the *S. alterniflora* removal projects. The specific objectives of this study are as follows: (1) to propose a new method considering the complex coastal environment and spectral features, to extract *S. alterniflora* with eight-band WV-2/3 imagery, (2) to extract *S. alterniflora* with Sentinel-1/2 imagery, and (3) to analyze the distribution changes of *S. alterniflora* based on the multi-temporal detection results.

## 2. Data

### 2.1. Study Site

The study area is located in Zhangjiangkou National Mangrove Nature Reserve, Zhangjiang Estuary, Fujian province, China (Figure 1). It is in the List of Wetlands of International Importance since 2008, protecting the northernmost and largest concentrated natural mangrove forests in China. Having been invaded by *S. alterniflora* for years, it is also a representative mangrove and *S. alterniflora* ectone [17]. The elevation of the study area is  $-6\sim 8$  m. The annual average temperature is  $21.2$  °C. The annual average rainfall is 1714.5 m. The annual average relative humidity is 79%.

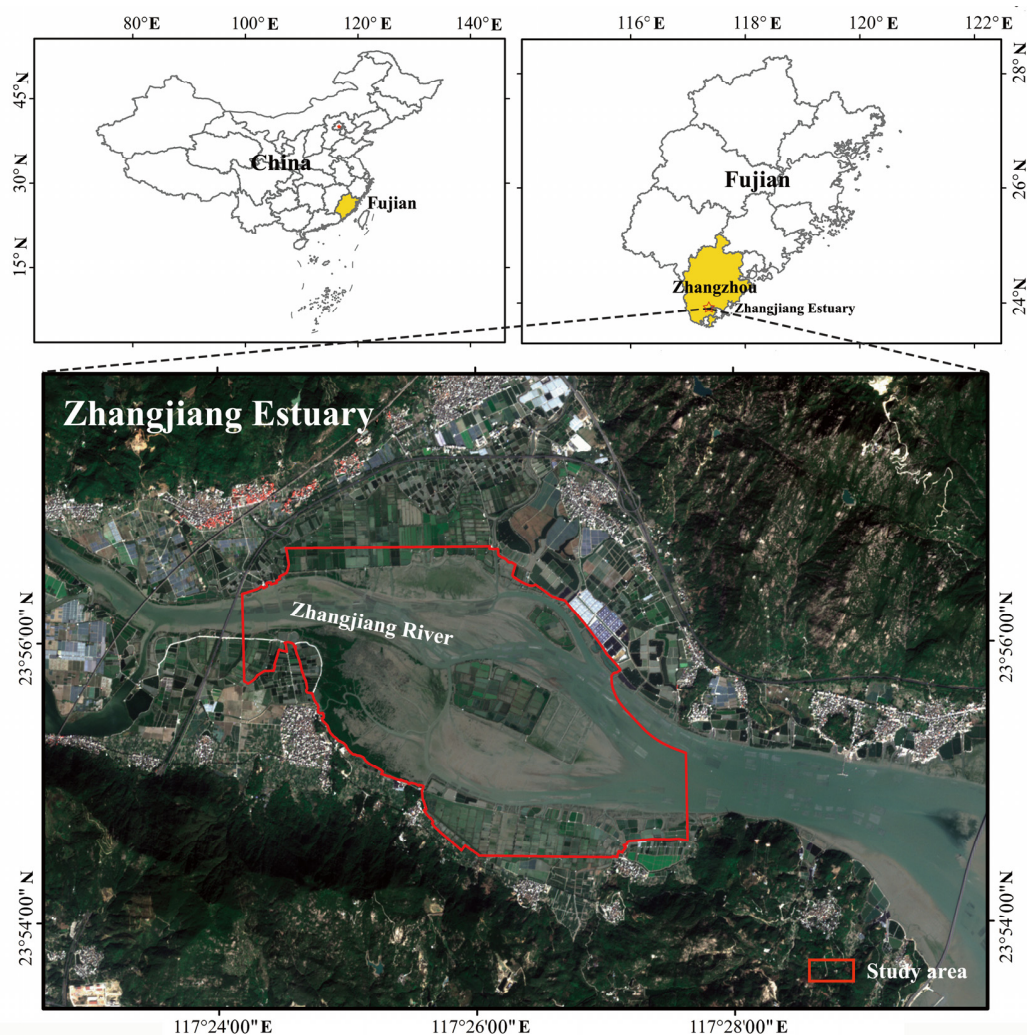


**Figure 1.** Location of the study site.

### 2.2. Data and Preprocessing

We acquired one WorldView-3 (WV-3) image on 17 October 2015 and one WorldView-2 (WV-2) image on 12 February 2017 to study the invasion process of *S. alterniflora*; one

Sentinel-2 image on 29 December 2023 and a Sentinel-1 time series acquired from March 2023 to March 2024 to monitor the *S. alterniflora* distribution after the *S. alterniflora* removal projects in Zhangjiang Estuary. The WV-2 and WV-3 images were Ortho-Ready Standard 2A products, which were geometrically corrected to WGS84 UTM Zone 50N. The WV-2 and WV-3 data were radiometrically corrected to reflectance at the top of the atmosphere. Atmospheric correction was then conducted with the Fast Line-of-site Atmospheric Analysis of Spectral Hypercubes (FLAASH) procedure in ENVI 5.3 and the parameters provided in the metadata file. The Sentinel-2 image was the Level-2A product which provided atmospherically corrected Surface Reflectance images. A total of 30 scenes of the Sentinel-1 C-band Ground Range Detected SAR imagery covering the study region were also collected. The SAR data are of the Interferometric Wide swath mode with dual-band vertical transmit/horizontal receive (VH) polarization and have a pixel size of 10 m. The boundary vector data of the study area were used to clip the images, masking out regions outside of the reserve (Figure 1).

### 2.3. Reference Data

To collect the reference data of different land covers (*S. alterniflora*, mangroves, mud flats, water, and algae), we carried out two field surveys in 2015 and 2017, gathered very high spatial resolution (VHR) UAV images [39] in 2015, 2017 and 2022, and accumulated two scenes of Beijing-3A satellite images [40] acquired on 19 December 2023 in Zhangjiang Estuary. We used in situ data derived from the field surveys and the Global Geo-Referenced Field Photo Library (<https://www.ceom.ou.edu/photos/> (accessed on 10 October 2019)), visually interpreted VHR images, and consultation information from local experts to create regions of interests (ROIs) for algorithm training and accuracy assessment.

## 3. Methods

### 3.1. A New Method to Extract *S. alterniflora* with 8-Band WV-2/3 Imagery

The procedure for *S. alterniflora* identification can be divided into three steps (Figure 2): (1) extraction of *S. alterniflora* and itinerant biological structures from water, mud flat and mangroves using the Ostu algorithm; (2) identification of vegetation from the itinerant biological structures with the SVM classifier; (3) discrimination of *S. alterniflora* from itinerant biological structures.

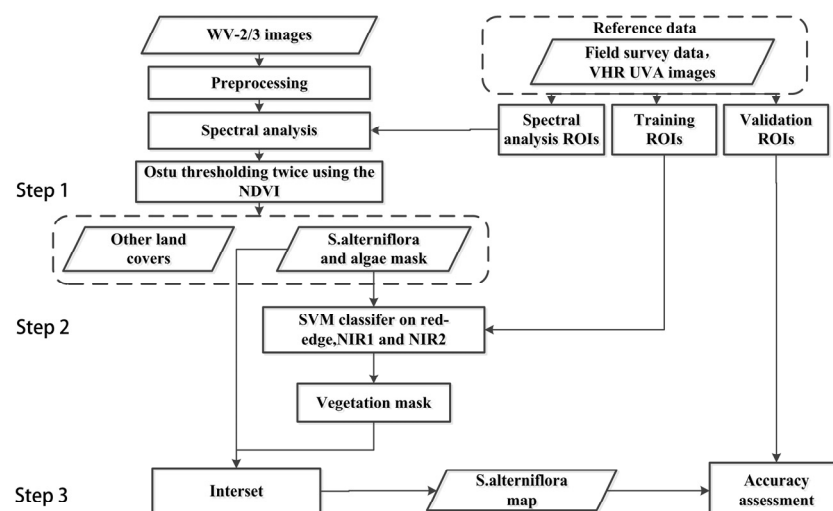


**Figure 2.** Flowchart of *S. alterniflora* detection based on 8-band WV-2/3 imagery.

#### 3.1.1. Spectral Analysis

After masking with the boundary vector data of the study area, the main land covers in the study region are water, mud flat, *S. alterniflora*, mangroves and itinerant biological structures. In the red-edge and two near-infrared bands, spectral responses were similar

between mud flats and algae but different between them and other land covers (Figure 3). Mud flats and algae were separable in the normalized difference vegetation index (NDVI) band, but the confusion between algae and *S. alterniflora* in the NDVI band was obvious (Figure 4). Thus, we first used NDVI to discriminate *S. alterniflora* from water, mud flats, and mangroves; then, we used the red-edge, NIR1, and NIR2 bands to distinguish *S. alterniflora* from algae.

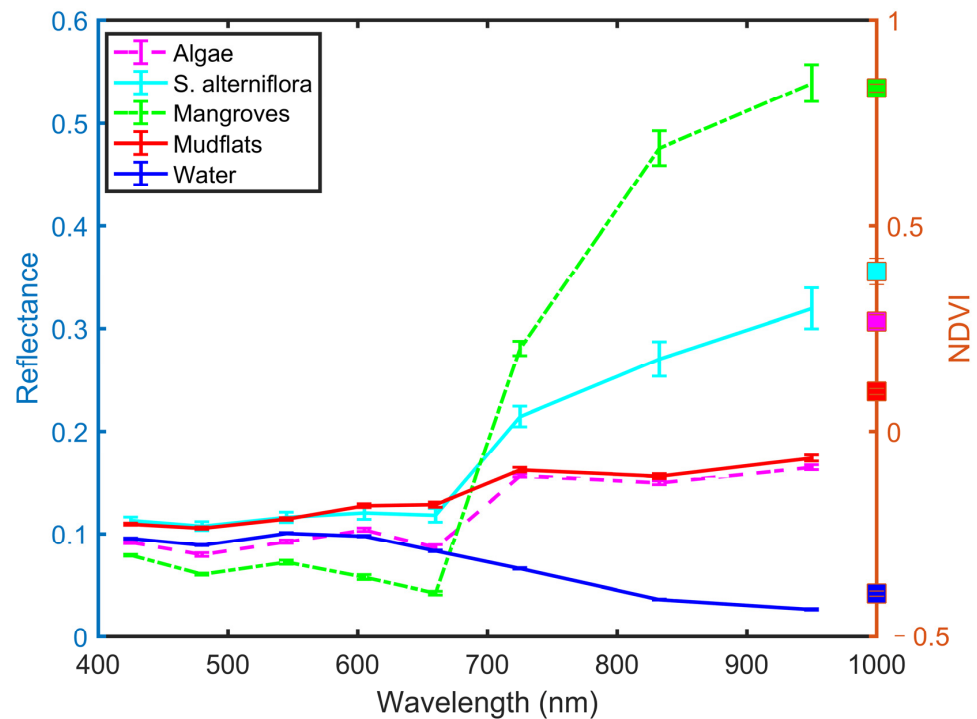


**Figure 3.** Reflectance and mean NDVI values of water, mud flat, *S. alterniflora*, mangroves and algae.

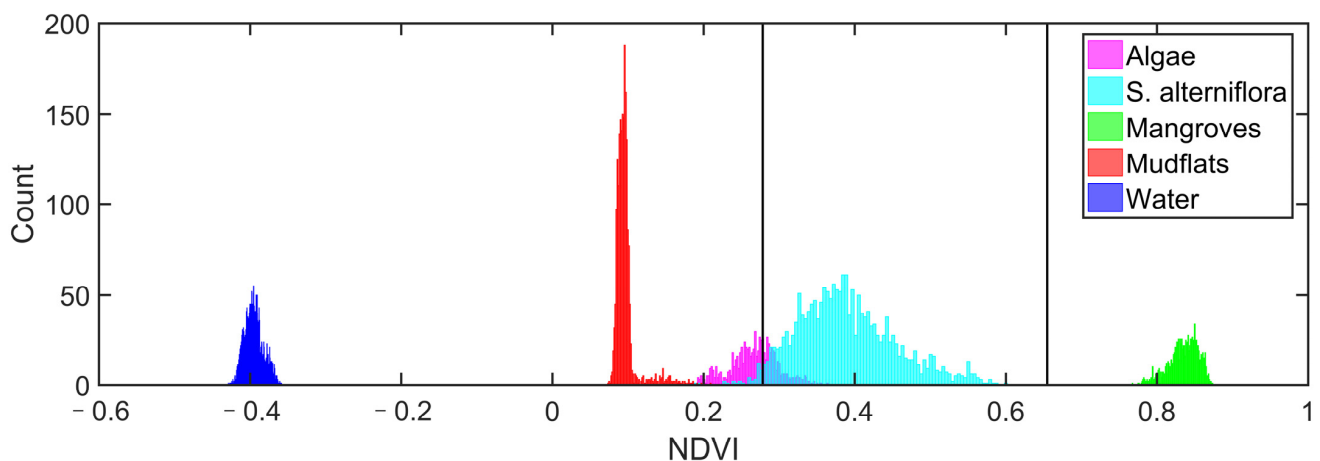


**Figure 4.** NDVI histograms of water, mud flats, *S. alterniflora*, mangroves and algae (the black lines denote the NDVI two-level thresholds with the Otsu algorithm in the study region).

### 3.1.2. The Extraction of *S. alterniflora* and Itinerant Biological Structures

Vegetation indices, such as NDVI [41], are widely used for vegetation mapping and monitoring [42]. Here, we combined Otsu thresholding [43] and NDVI to extract *S. alterniflora* and itinerant biological structures. The Otsu algorithm automatically find the optimal threshold to segment the image into two classes by maximizing inter-class variances [44]. We first applied Otsu thresholding to the NDVI image (Figure 5a) and obtained a binary

classification of vegetation and non-vegetation (Figure 5b). The vegetation mask had at least three land cover types—mangroves, *S. alterniflora* and itinerant biological structures, which were separated in NDVI values (Figure 5b). Then, we computed 2-level thresholds based on the vegetation NDVI image using the Otsu algorithm and selected the larger NDVI threshold to obtain the mangrove mask (Figure 5c) and the mask which contains *S. alterniflora* and algae only (Figure 5d).

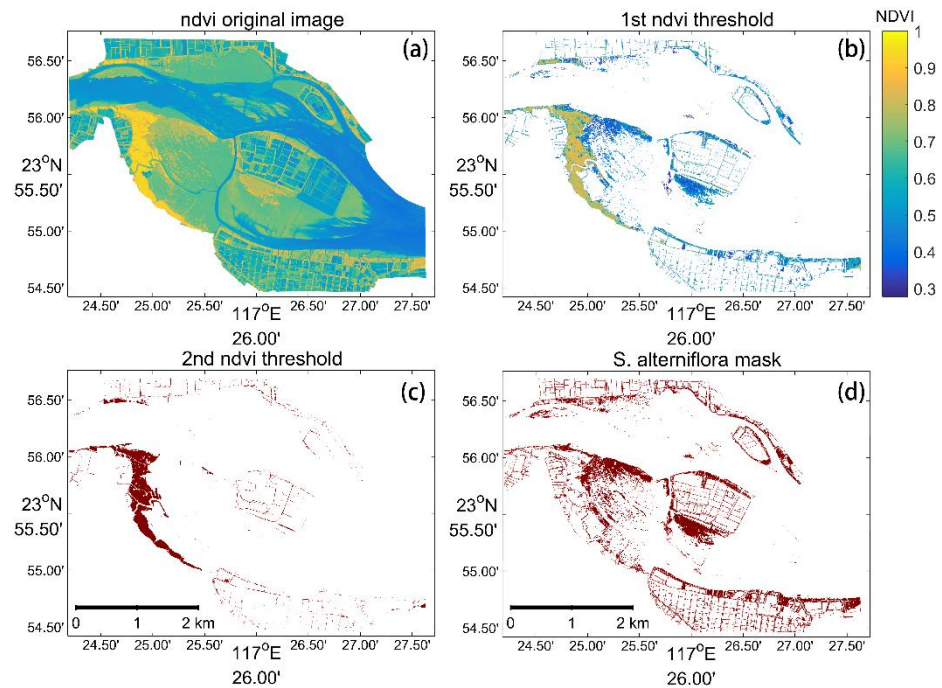


**Figure 5.** NDVI of the study region (a), the remained NDVI data after the 1st Otsu thresholding (b), the remained NDVI mask after the 2nd Otsu thresholding (c), the mask of *S. alterniflora* and algae (d).

### 3.1.3. Discrimination of *S. alterniflora* from Itinerant Biological Structures

To discriminate vegetation from algae, we applied the SVM classifier to the image of red-edge, NIR1, and NIR2 bands, and we obtained a binary classification result of vegetation and non-vegetation (Figure S1). SVM [45] is a supervised non-parametric statistical learning technique [46], which has been widely used in remote sensing applications [46,47]. It aims to find an optimal hyperplane that separates the samples of vegetation and non-vegetation classes and also minimizes misclassifications [48]. SVM has been regarded as a promising algorithm due to the good performance with limited training samples and the lower sensitivity to the curse of dimensionality compared with traditional classifiers [46]. In this study, we used the radial basis function kernel for SVM. The parameters gamma and penalty are set to be 0.333 and 100, respectively. In order to reduce the impact of algae, which displays similar spectral signals with *S. alterniflora*, we intentionally selected some mud flats covered by algae as the non-vegetation samples by visual interpretation of the VHR images. To further discriminate *S. alterniflora* from algae, we intersected the *S. alterniflora* and algae mask with the vegetation mask, manually deleted the patches located on the land, and obtained the final *S. alterniflora* distribution data.

### 3.2. Intra-Class Separability Evaluation

We employed the Jeffries–Matusita ( $J-M$ ) distance to quantify the respective spectral separability between different land covers [20]. The  $J-M$  distance has upper and lower bounds which vary between 0 and  $\sqrt{2}$  [49,50]. The higher  $J-M$  values indicate larger inter-class distances between *S. alterniflora* and other land covers, which benefits the *S. alterniflora* detection. The formula of the  $J-M$  distance is listed as follows:

$$\alpha = \frac{1}{8}(\mu_i - \mu_j)^T \left( \frac{C_i + C_j}{2} \right)^{-1} (\mu_i - \mu_j) + \frac{1}{2} \ln \left( \frac{(|C_i + C_j|/2)}{\sqrt{|C_i| \times |C_j|}} \right) \tag{1}$$

$$JM_{ij} = \sqrt{2(1 - e^\alpha)} \tag{2}$$

where  $i$  and  $j$  are the two classes being compared,  $C_i$  is the covariance matrix of signature  $i$ , and  $\mu_i$  denotes the mean vector of signature  $i$ .

### 3.3. The Method to Extract *S. alterniflora* with Sentinel-1/2 Imagery

Due to the frequent cloud cover along the coastlines, the long revisit time of high-resolution satellite sensors as well as the short-duration *S. alterniflora* removal projects, we directly used the Sentinel-1 and Sentinel-2 satellite imagery to monitor the *S. alterniflora* distribution changes after the removal projects at the end of 2023. The hierarchical classification framework [17] was applied to detect *S. alterniflora* (Figure 6). Tidal inundation is an important factor which impacts the survival and reproduction of mangroves and salt marshes [18,51,52]. We used the Sentinel-1 SAR image time series from March 2023 to March 2024 to produce the inundation frequency map  $F_{VH < -19}$ . And  $F_{VH < -19} < 90\%$  was applied to obtain the mask of potential areas of mangroves and *S. alterniflora* (Figure S2). Then, we used the random forest classifier to classify the Sentinel-2 image on 29 December 2023 into different land covers including water, mud flats, mangroves, *S. alterniflora* and other vegetation. The input data of the classifier include spectral and texture features. The spectral features include the red, green, blue, NIR and SWIR bands, normalized difference water index (NDWI) [41], modified normalized difference water index (mNDWI) [53], NDVI, enhanced vegetation index (EVI) [54], and land surface water index (LSWI) [55]. The texture feature is the standard deviation of NDVI in a box with a radius of 5 pixels. We used the potential areas of mangroves and *S. alterniflora* to mask the spectral and texture features before classification. As for the random forest classifier, the number of trees was 100, and the number of variables per split was the square root of the number of variables. We manually deleted the patches located on the land to obtain the *S. alterniflora* distribution data.

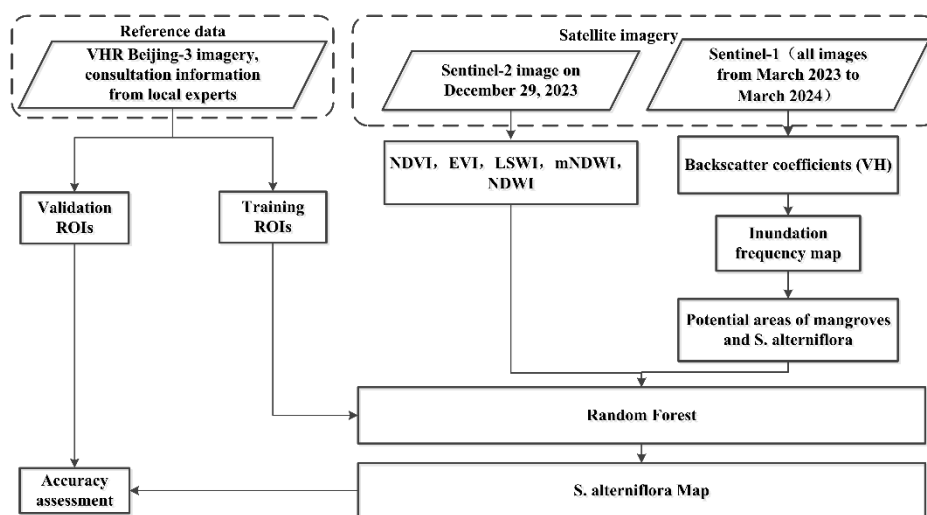


Figure 6. Flowchart of *S. alterniflora* detection based on Sentinel-1/2 imagery.

### 3.4. Accuracy Assessment

For validation, a total of 300 pixels were selected for 2 classes, namely *S. alterniflora* and other land covers, through stratified equalized random sampling [56]. We quantified the classification accuracy using overall accuracy (OA), confusion matrix, user accuracy, and producer accuracy. The SVM classifier was also used to identify four land covers including

*S. alterniflora*, mangroves, mud flats, and water in the study region, for performance comparison with the method to extract *S. alterniflora* with eight-band WV-2/3 imagery. The input features of the SVM classifier were the eight spectral bands of the WV imagery.

## 4. Results

### 4.1. Intra-Class Separability Statistics

Figure 7 shows spectral separability statistics between *S. alterniflora* and mangroves, mud flats, water, and algae. For *S. alterniflora* and algae, the *J-M* distance values were relatively high (greater than 1.40) in the NIR1 and NIR2 bands, and they remained low (smaller than 1.10) in the NDVI band. This is consistent with the reflectance statistics in Figure 3, suggesting the spectral mixtures of *S. alterniflora* and algae in the NDVI band and the importance of NIR1 and NIR2 bands for *S. alterniflora* detection. In addition, the *J-M* distance values were all greater than 1.40 in the NDVI band for *S. alterniflora* and mangroves, *S. alterniflora* and mud flats, as well as *S. alterniflora* and water, which also implies the effectiveness of NDVI to detect *S. alterniflora* from water, mud flats, and mangroves. For *S. alterniflora* and mud flats, as well as *S. alterniflora* and water, the *J-M* distance values were higher in the red-edge, NIR1, NIR2 and NDVI bands compared with those in the coastal, blue, green, yellow and red bands, which indicates that those bands are more suitable for distinguishing *S. alterniflora* from mud flats or water. Thus, the intra-class separability statistics here proved the reliability of the band selection in our proposed method to extract *S. alterniflora* with eight-band WV-2/3 imagery in Section 3.1.

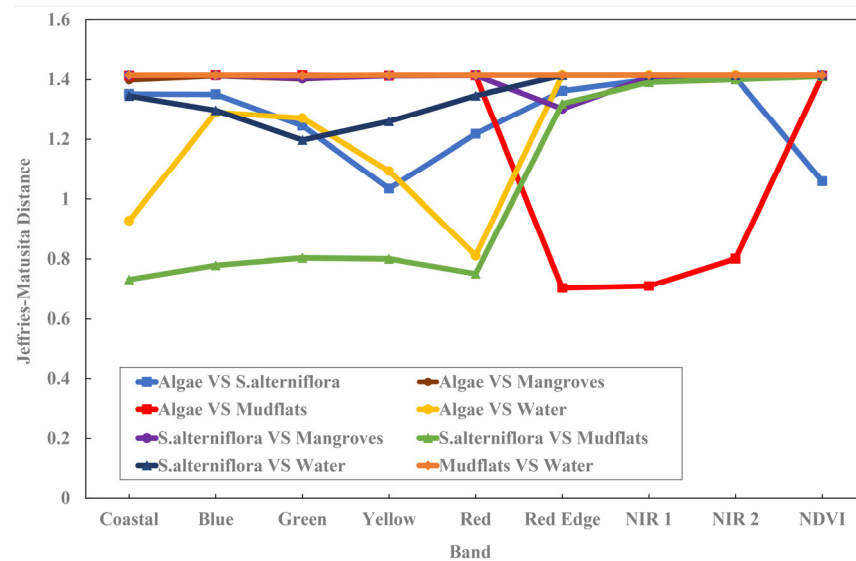


**Figure 7.** *J-M* distance values of different land covers. Coastal, blue, green, yellow, red, red-edge, NIR1, and NIR2 bands correspond to the eight spectral bands of the WV-2/3 satellite imagery.

### 4.2. *S. alterniflora* Detection Results

Table 1 presents *S. alterniflora* identification accuracies with the proposed method to extract *S. alterniflora* with eight-band WV-2/3 imagery and the traditional SVM classifier. Compared with the SVM classifier (OA = 82% in 2015 and 85% in 2017), our proposed method achieved higher identification accuracies of *S. alterniflora* (OA = 95% in 2015 and 93% in 2017). And the overall accuracies were significantly different between the proposed method and the SVM classifier based on the ANOVA test ( $p < 0.05$ ). The poorest accuracy was obtained using SVM and all eight spectral bands of WV-3 imagery, and it was due to higher *S. alterniflora* omission errors (Table 1). It also showed the better *S. alterniflora* detection results of our proposed method.

The confusion matrix shows that our detection results are consistent with validation samples. As illustrated in Figure 8a–d, the shapes and boundaries of the *S. alterniflora*

patches are in accordance with the WV-2/3 imagery, and the small *S. alterniflora* patches are precisely detected and separated from the mud flats and algae. The OA of *S. alterniflora* detection based on Sentinel-1/2 imagery is greater than 90%, which suggests the reliability of the detection results. The *S. alterniflora* area was 115.19 hm<sup>2</sup> in 2015, 152.40 hm<sup>2</sup> in 2017 and 15.29 hm<sup>2</sup> in 2023, respectively (Figure 8). Our result in 2015 was close to the area derived by Liu et al. [15] (116.11 hm<sup>2</sup>) with high-resolution GE imagery in 2015.

**Table 1.** Confusion matrix of *S. alterniflora* detection using the proposed method and SVM classifier with WV-2/3 imagery.

Method	Year	Class	SA	Non-SA	Use. Acc.	OA
Our method	2015	SA	134	16	89%	95%
		Non-SA	0	150	100%	
		Pro. acc.	100%	90%		
SVM	2015	SA	98	52	65%	82%
		Non-SA	1	149	99%	
		Pro. acc.	99%	88%		
Our method	2017	SA	130	20	87%	93%
		Non-SA	1	149	99%	
		Pro. acc.	99%	88%		
SVM	2017	SA	100	50	67%	83%
		Non-SA	0	150	100%	
		Pro. acc.	100%	75%		

Notes: SA denotes *S. alterniflora*, non-SA denotes non-*S. alterniflora* land covers, Use. acc. denotes user accuracy, and Pro. acc. denotes producer accuracy.

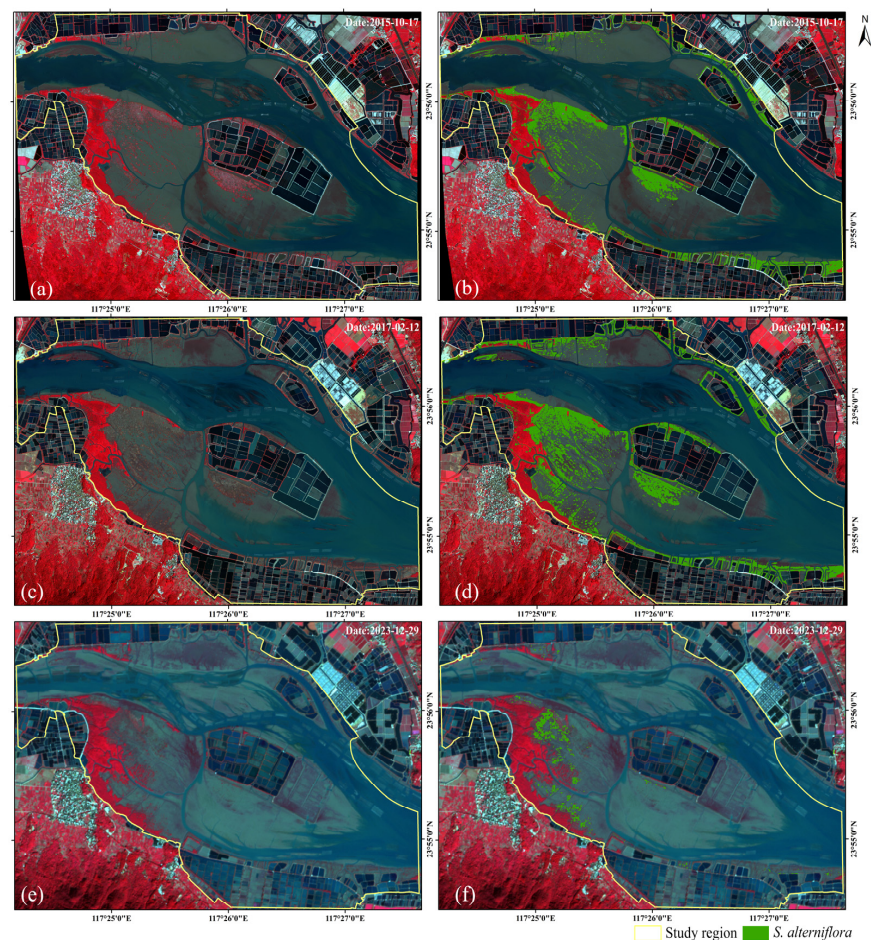


**Figure 8.** The WV-3 image (a) and detected *S. alterniflora* on 17 October 2015 (b), the WV-2 image (c) and detected *S. alterniflora* on 12 February 2017 (d); the Sentinel-2 image (e) and detected *S. alterniflora* on 29 December 2023 (f).

#### 4.3. The *S. alterniflora* Distribution Changes from 2015 to 2023

The *S. alterniflora* area in the study area increased from 115.19 hm<sup>2</sup> in 2015 to 152.40 hm<sup>2</sup> in 2017, but it decreased dramatically to 15.29 hm<sup>2</sup> in 2023. Figure 9 shows clearly the extensive expansion of *S. alterniflora* from 2015 to 2017, and the newly colonized *S. alterniflora* clumps of small sizes were evidently spread on the mud flats in the east of the study region. From 2015 to 2017, *S. alterniflora* expanded at a rate of 27.91 hm<sup>2</sup>/a, which was similar to Liu et al. [15]. The large-scale *S. alterniflora* losses from 2017 to 2023 (Figure 9) showed that the local *S. alterniflora* removal projects have achieved remarkable achievements.

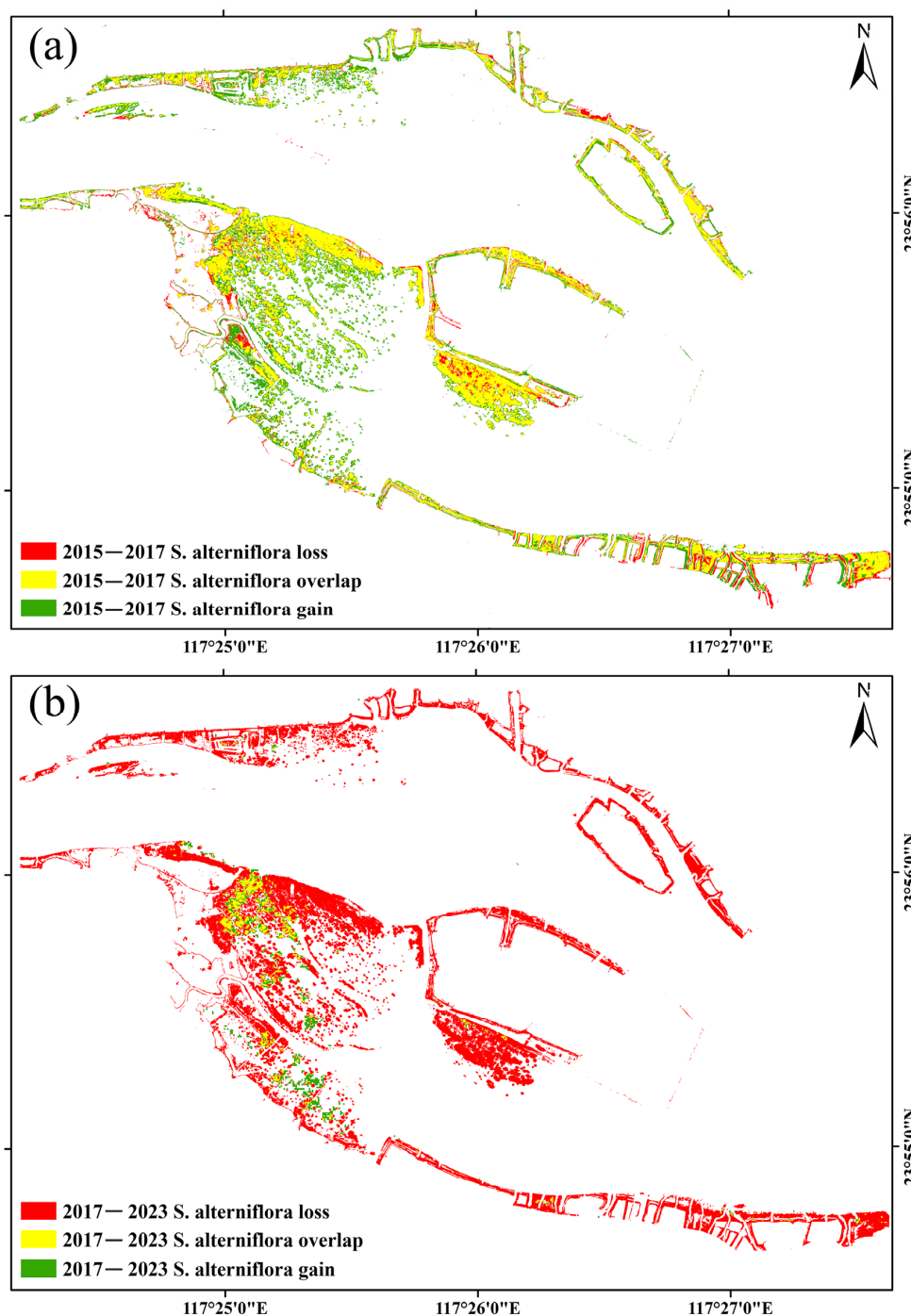


Figure 9. The gains and losses of *S. alterniflora* from 2015 to 2017 (a) and from 2017 to 2023 (b).

## 5. Discussion

### 5.1. Adaptability of the Method and Data

In this study, we explored the synergistic use of WV-2/3 and Sentinel-1/2 images to monitor gains and losses of *S. alterniflora* in Zhangjiang Estuary. The high spatial resolution WV-2/3 satellite imagery has clear advantages in detecting *S. alterniflora* at a fine scale, such as accurately monitoring the growth of the newly colonized clumps and the invasion process. Researchers have recommended high spatial resolution GE imagery for the *S. alterniflora* monitoring [15], but the GE imagery only has three bands, which may lead to spectral confusions of different land covers, such as algae and *S. alterniflora* in the coastal areas [31]. The overall accuracies reported by Liu et al. [15] based on GE images were not greater than 90%, which is lower than the accuracy achieved by our method (Table 1). Here, we take advantage of the multispectral information, especially the red-edge, NIR1, and NIR2 bands of WV-2/3 imagery to separate *S. alterniflora* from algae on the mud flats. In contrast with the traditional SVM method, our proposed method shows a significantly higher accuracy of *S. alterniflora* detection. Moreover, previous researchers usually classified all the land covers [15,16], which needed a large amount of training sample data and computation time. Our method based on WV-2/3 imagery mainly consists of Otsu thresholding and the SVM classifier, and the SVM classifies the study region into two classes, i.e., vegetation and non-vegetation, which requires less training samples and computation cost.

Similar to the method proposed by Dong et al. [17], we used Sentinel-1 SAR time series to calculate the inundation frequency map and obtained the mask of potential areas of mangroves and *S. alterniflora* for further identification. Dong et al. [17] have shown that the inundation frequency mask can efficiently delete areas where ephemeral structures such as algae exist and maintain areas where *S. alterniflora* and mangroves persist. Thus, we provide two solutions here to discriminate *S. alterniflora* from algae on the mud flats with remote sensing imagery. The first solution is to utilize red-edge, NIR1, and NIR2 bands to detect vegetation from algae; and the second solution is to employ an inundation frequency map derived from SAR time series to delete algae. The main reasons we used an inundation frequency map to limit the impact of algae on *S. alterniflora* detection results with Sentinel-2 imagery are (1) the spatial resolution of Sentinel-2 imagery makes it difficult to collect pure algae samples compared with that using WV-2/3 imagery and (2) freely accessible Sentinel-1 SAR data have been widely used in synergy with Sentinel-2 imagery for nature resource monitoring [17,57–59].

Due to the high frequency of cloud cover and tidal inundation, we resorted to Sentinel-1/2 imagery to monitor the effectiveness of *S. alterniflora* removal projects. Researchers have already utilized medium spatial resolution satellite imagery, such as Landsat and Sentinel, to monitor *S. alterniflora* removal projects [9,13]. Zhang et al. [9] quantified the expansion and removal of *S. alterniflora* on Chongming island, China, with multi-temporal Landsat images from 1995 to 2018, while the in situ field survey was carried out in 2012 and 2015. Min et al. [13] identified the *S. alterniflora* removal event and the corresponding removal timing based on Sentinel-2 and Landsat-8 imagery in Shandong Province and Fujian Province, China. Due to the difficulty collecting a large amount of field observation data, Min et al. [13] conducted field investigations in the Yangtze River Delta, Shandong Province by using a GPS unit and collecting UAV imagery, and they also analyzed the VHR PlanetScope images for validation. Field surveys can provide valuable information for *S. alterniflora* investigation, and researchers collected field survey data for the training and validation of the remote sensing method. But the time and labor required to conduct a comprehensive survey may limit the extent and number of the surveys. In addition, it may be difficult or even dangerous to conduct in situ surveys in some inaccessible coastal areas. Due to the scarcity of field survey data, researchers also relied on VHR remote sensing data for validation [13,34,38]. In this study, we combined the method of using VHR Beijing-3A satellite imagery and consulting with local experts to validate the *S. alterniflora* distribution maps derived from Sentinel-2 imagery acquired in December 2023. By comparing the

Beijing-3A satellite imagery acquired in 2023 and the UAV imagery acquired in 2022 (Figures 10 and 11), we found that the spatial resolution of the remote sensing imagery and the mangrove and *S. alterniflora* ectone environment make it challenging to distinguish *S. alterniflora* from the newly grown mangrove trees using Sentinel-2 imagery. For example, Figure 10A,C show the coexistence of newly grown mangrove trees (dark green and rough patches) and *S. alterniflora* (light green and smooth patches) when the removal projects have not been implemented in 2022. Figure 11A,C show clearly the remaining young mangrove trees, while *S. alterniflora* has been mostly removed in December 2023. By comparing Figures 10B and 11B, we can see the remaining *S. alterniflora* in 2023 (the *S. alterniflora* eradication project was still underway at that time). In Figure 11A,C, the spectral mixtures of young mangrove trees and mud flats make the spectral signals similar to *S. alterniflora* on Sentinel-2 imagery (Figure S3), which resulted in their misclassification. However, the outstanding achievements of the *S. alterniflora* removal projects in 2023 are obvious by a comparison of WV-2/3 imagery and Sentinel-2 imagery from 2015 to 2023.

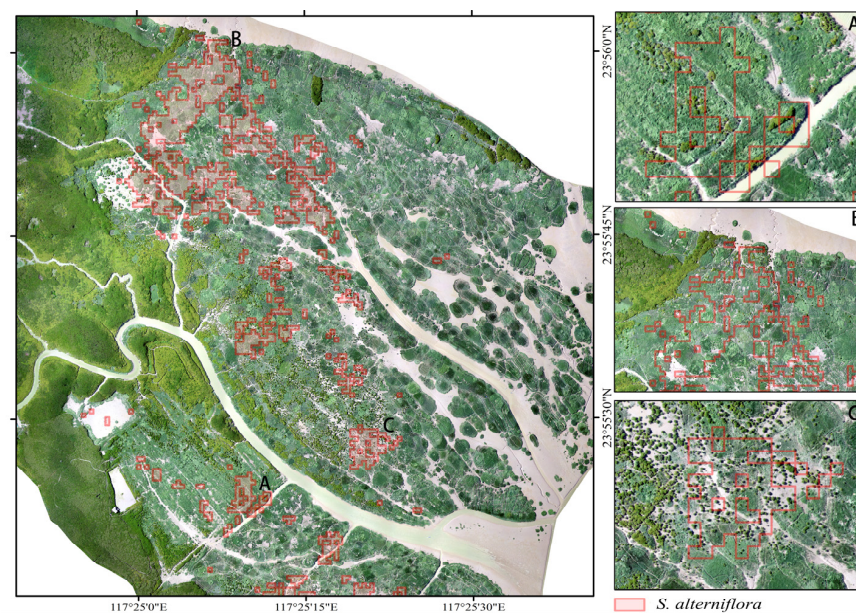


**Figure 10.** The *S. alterniflora* distribution results derived from Sentinel-1/2 imagery on 29 December 2023 overlaid on the UAV imagery acquired in June 2022. (A–C) on the right are the enlarged views of the figure on the left.

Many researchers have compared Sentinel-2 and WV-3 imagery for wetland mapping [60,61]. WV-3 is a commercial satellite with eight bands at a 2 m spatial resolution in the visible and near-infrared spectrum, but data catalogs are expensive and limited in scope [60]. Sentinel-2 offers a global, freely available dataset where four bands are of 10 m spatial resolution in the visible and near-infrared spectrum [60]. Researchers concluded that WV-3 could provide nature resource maps with more detail and higher classification accuracy values in comparison with the classification results derived from Sentinel-2 imagery [62,63]. Similarly, the *S. alterniflora* detection maps derived from WV-2/3 imagery (Figure 8) provide better *S. alterniflora* delineation than the Sentinel-2 based *S. alterniflora* map here. Although limited by the spatial resolution, Sentinel-2 can still effectively present the *S. alterniflora* removals in the study region (Figures 8 and 9). Moreover, researchers [13] investigated the automatic and rapid detection of *S. alterniflora* removal events at a large scale with Sentinel-2 and Landsat-8 time-series data. They showed good accuracies for removal detection in Fujian Province and Shandong Province [13]. As many large-scale short-term *S. alterniflora* removal projects have been enacted in China, Sentinel-2 provides a good data source for monitoring these kinds of large-scale *S. alterniflora* distribution changes. But the spatial resolution of the remote sensing data is still limited for distin-

guishing young mangrove trees. *S. alterniflora*, WV-3 or other VHR remote sensing data would be better choices for monitoring early-stage invasion and the re-invasion process of *S. alterniflora*.

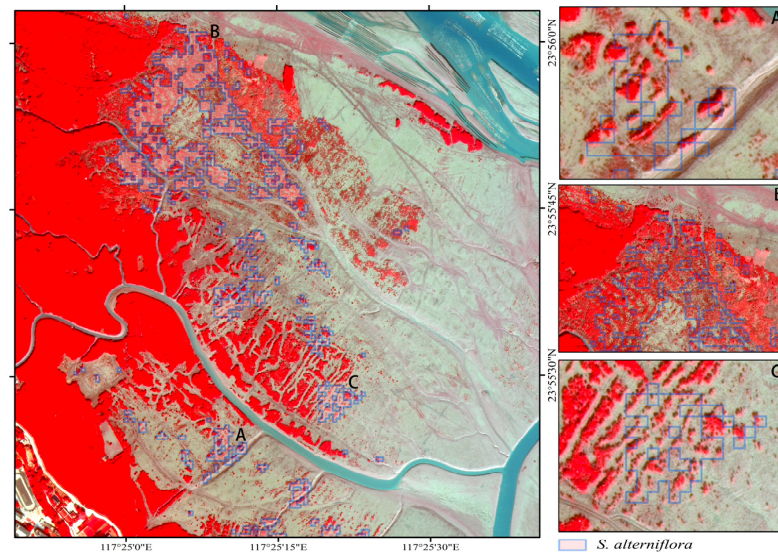


**Figure 11.** The *S. alterniflora* distribution results derived from Sentinel-1/2 imagery on 29 December 2023 overlaid on the Beijing-3A satellite imagery acquired on 19 December 2023. (A–C) on the right are the enlarged views of the figure on the left.

### 5.2. The Expansion and Removal of *S. alterniflora* in Zhangjiang Estuary

*S. alterniflora* can reproduce both sexually and asexually [64,65]. They spread by seed, rhizome, or vegetative fragmentation [66]. The *S. alterniflora* detection results from 2015 to 2017 (Figure 12) clearly suggest that the clonal growth of *S. alterniflora* mainly contribute to its area increase. The expansion of isolated *S. alterniflora* patches in the study region is consistent with the results based on multi-temporal UAV imagery from Zhu et al. [18]. And this suggests that the VHR WV-2/3 imagery provides a valuable supplement to *S. alterniflora* remote sensing monitoring. The large-scale *S. alterniflora* eradication project is at an advanced stage, with a removal rate of about 90% in Zhangjiang Estuary, which is in line with the conclusions from Min et al. [13].

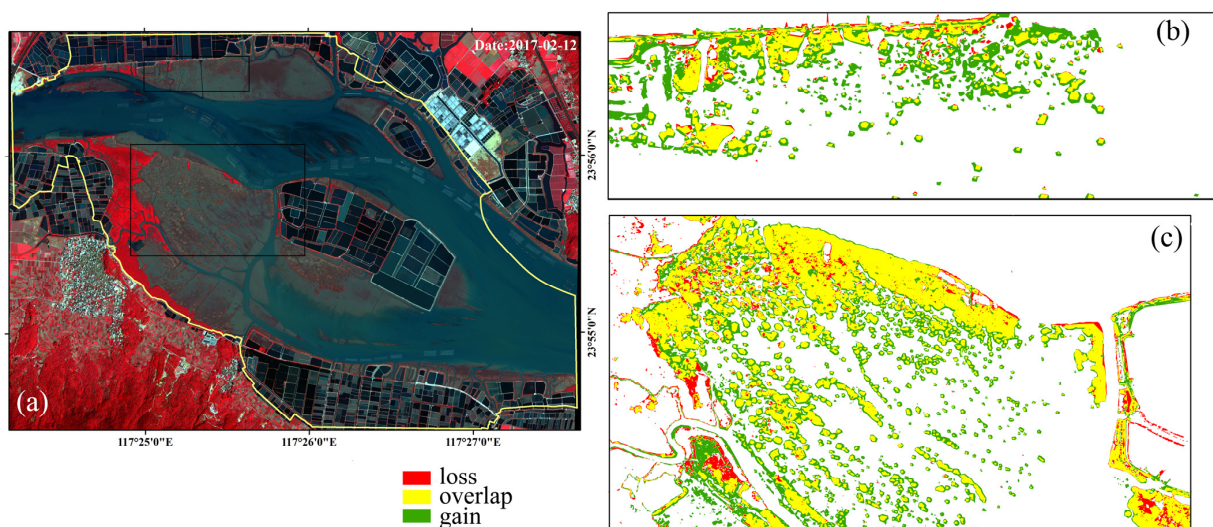


**Figure 12.** The overview of the WV-2 image (a); the corresponding enlarged views of *S. alterniflora* distribution changes (b,c) in the two rectangles of the overview figure from 2015 to 2017.

### 5.3. Implications for *S. alterniflora* Control and Management

Biological invasion is a significant component of human-caused global environmental change [67]. *S. alterniflora*, native to the East and Gulf Coasts of North America, has caused considerable ecological and economic damages [68,69]. Due to its high reproductive ability and strong adaptability to adverse environmental factors such as elevated salinity [70], *S. alterniflora* has become one of most important invasive salt marshes, threatening China's coastal wetlands [6,71]. Given the negative effects, high dispersal ability and reinvasion potential of *S. alterniflora*, China has issued the "Special Action Plan for the Prevention and Control of *Spartina Alterniflora* (2022–2025)". By 2025, the *S. alterniflora* area will continue to decline and may even disappear under the strong policy promotion [14,21]. To evaluate the effectiveness of the *S. alterniflora* removal and control projects, we need methods that monitor the *S. alterniflora* distribution changes in a timely manner [13]. This study proposes a framework to combine multi-source high and medium spatial resolution satellite imagery to monitor *S. alterniflora* distributions before and after the removal projects. Researchers have concluded that it is difficult to eradicate *S. alterniflora* in the short term: the seeds transporting via the tides and ocean currents as well as residual roots in the soil make *S. alterniflora* reinvasion in the following year highly possible [13,72]. And the low vegetation coverage and biomass of the newly grown *S. alterniflora* after the first removal event make it challenging to continuously monitor and assess the effectiveness of the *S. alterniflora* eradication projects [13]. So besides capturing the first removal event, the continuous high-spatial resolution monitoring of *S. alterniflora* is quite essential to control secondary invasion and restore coastal wetlands.

## 6. Conclusions

In this study, we combined multi-temporal WV-2/3 and Sentinel 1/2 imagery to monitor *S. alterniflora* dynamics before and after the *S. alterniflora* removal projects. We put forward a new method for *S. alterniflora* detection with eight-band WV-2/3 imagery. The proposed method first used NDVI to discriminate *S. alterniflora* from water, mud flats and mangroves based on Ostu thresholding, and then we used the red-edge, NIR1 and NIR2 bands and SVM classifier to distinguish *S. alterniflora* from algae. Due to the contamination of frequent cloud cover and tidal inundation, the long revisit time of high-resolution satellite sensors and the short-term *S. alterniflora* removal projects, we combined Sentinel-1 SAR time series and Sentinel-2 optical imagery to monitor the *S. alterniflora* removal project status in 2023. The overall accuracies of the *S. alterniflora* detection results here are all greater than 90%. Compared with the traditional SVM method, the proposed method achieved a higher identification accuracy of *S. alterniflora*. The *S. alterniflora* area was 115.19 hm<sup>2</sup> in 2015, 152.40 hm<sup>2</sup> in 2017 and 15.29 hm<sup>2</sup> in 2023, respectively. The generated *S. alterniflora* maps clearly show the clonal growth of *S. alterniflora* in Zhangjiang Estuary from 2015 to 2017. And the large-scale *S. alterniflora* eradication project has achieved remarkable results with a removal rate of about 90% in Zhangjiang Estuary. With the continuous implementation of the "Special Action Plan for the Prevention and Control of *Spartina Alterniflora* (2022–2025)" in China, continual high-spatial resolution monitoring of *S. alterniflora* is significant to control secondary invasion and restore coastal wetlands.

**Supplementary Materials:** The following supporting information can be downloaded at <https://www.mdpi.com/article/10.3390/w16131780/s1>, Figure S1: The detected vegetation map from the SVM classifier with WV-2 image acquired on 12 February 2017; Figure S2: The inundation frequency map (a) and the inundation frequency mask (b); Figure S3: The *S. alterniflora* distribution results derived from Sentinel-1/2 imagery overlaid on the Sentinel-2A satellite imagery acquired on 29 December 2023. A, B and C on the right are the enlarged views of the figure on the left.

**Author Contributions:** D.D.: conceptualization, data collection, formal analysis, visualization, and writing—original draft. H.H.: validation, formal analysis, writing—review and editing, supervision, and funding acquisition. Q.G.: visualization and formal analysis. All authors have read and agreed to the published version of the manuscript.

**Funding:** This work was supported by the Marine Economy Special Project of the Guangdong Province (GDNRC[2024]36); the Director’s Foundation of South China Sea Bureau of Ministry of Natural Resources (230206); the Science and Technology Project of Guangdong Forestry Administration (2024): Monitoring and Ecological Value Assessment of Coastal Wetland Resources in the Guangdong Province, the Science and Technology Project of Guangdong Forestry Administration (2023): Research on Carbon Storage Verification, Potential Assessment and Carbon Sink Trading Mechanism of Typical Coastal Wetlands.

**Data Availability Statement:** The authors confirm that the data supporting the findings of this study are available within the article. The Sentinel imagery is available in the public domain: <https://dataspace.copernicus.eu/> (accessed on 20 March 2024).

**Acknowledgments:** Thanks to the reviewers and editors for their valuable suggestions on this paper.

**Conflicts of Interest:** The authors declare no conflicts of interest.

## References

- Zhang, D.; Hu, Y.; Liu, M.; Chang, Y.; Yan, X.; Bu, R.; Zhao, D.; Li, Z. Introduction and spread of an exotic plant, *Spartina alterniflora*, along coastal marshes of China. *Wetlands* **2017**, *37*, 1181–1193. [CrossRef]
- Valiela, I.; Fox, S.E. Managing coastal wetlands. *Science* **2008**, *319*, 290–291. [CrossRef] [PubMed]
- Barbier, E.B.; Hacker, S.D.; Kennedy, C.; Koch, E.W.; Stier, A.C.; Silliman, B.R. The value of estuarine and coastal ecosystem services. *Ecol. Monogr.* **2011**, *81*, 169–193. [CrossRef]
- Duarte, C.M.; Losada, I.J.; Hendriks, I.E.; Mazarrasa, I.; Marbà, N. The role of coastal plant communities for climate change mitigation and adaptation. *Nat. Clim. Change* **2013**, *3*, 961–968. [CrossRef]
- Shepard, C.C.; Crain, C.M.; Beck, M.W. The protective role of coastal marshes: A systematic review and meta-analysis. *PLoS ONE* **2011**, *6*, e27374. [CrossRef] [PubMed]
- Wang, X.; Xiao, X.; He, Q.; Zhang, X.; Wu, J.; Li, B. Biological invasions in China’s coastal zone. *Science* **2022**, *378*, 957. [CrossRef]
- Zhang, X.; Xiao, X.; Wang, X.; Xu, X.; Qiu, S.; Pan, L.; Ma, J.; Ju, R.; Wu, J.; Li, B. Continual expansion of *Spartina alterniflora* in the temperate and subtropical coastal zones of China during 1985–2020. *Int. J. Appl. Earth Obs.* **2023**, *117*, 103192. [CrossRef]
- Zhang, X.; Xiao, X.; Qiu, S.; Xu, X.; Wang, X.; Chang, Q.; Wu, J.; Li, B. Quantifying latitudinal variation in land surface phenology of *Spartina alterniflora* saltmarshes across coastal wetlands in China by Landsat 7/8 and Sentinel-2 images. *Remote Sens. Environ.* **2022**, *269*, 112810. [CrossRef]
- Zhang, X.; Xiao, X.; Wang, X.; Xu, X.; Chen, B.; Wang, J.; Ma, J.; Zhao, B.; Li, B. Quantifying expansion and removal of *Spartina alterniflora* on Chongming island, China, using time series Landsat images during 1995–2018. *Remote Sens. Environ.* **2020**, *247*, 111916. [CrossRef]
- Mao, D.; Liu, M.; Wang, Z.; Li, L.; Man, W.; Jia, M.; Zhang, Y. Rapid Invasion of *Spartina alterniflora* in the Coastal Zone of Mainland China: Spatiotemporal Patterns and Human Prevention. *Sensors* **2019**, *19*, 2308. [CrossRef]
- Zhou, J.; Zhang, J.; Chen, Y.; Qin, G.; Cui, B.; Lu, Z.; Wu, J.; Huang, X.; Thapa, P.; Li, H. Blue carbon gain by plant invasion in saltmarsh overcompensated carbon loss by land reclamation. *Carbon Res.* **2023**, *2*, 39. [CrossRef]
- Wan, S.; Qin, P.; Liu, J.; Zhou, H. The positive and negative effects of exotic *Spartina alterniflora* in China. *Ecol. Eng.* **2009**, *35*, 444–452. [CrossRef]
- Min, Y.; Cui, L.; Li, J.; Han, Y.; Zhuo, Z.; Yin, X.; Zhou, D.; Ke, Y. Detection of large-scale *Spartina alterniflora* removal in coastal wetlands based on Sentinel-2 and Landsat 8 imagery on Google Earth Engine. *Int. J. Appl. Earth Obs.* **2023**, *125*, 103567. [CrossRef]
- Zhao, W.; Li, X.; Xue, L.; Lin, S.; Ma, Y.; Su, L.; Li, Z.; Gong, L.; Yan, Z.; Macreadie, P.I. Mapping trade-offs among key ecosystem functions in tidal marsh to inform spatial management policy for exotic *Spartina alterniflora*. *J. Environ. Manag.* **2023**, *348*, 119216. [CrossRef] [PubMed]
- Liu, M.; Li, H.; Li, L.; Man, W.; Jia, M.; Wang, Z.; Lu, C. Monitoring the invasion of *Spartina alterniflora* using multi-source high-resolution imagery in the Zhangjiang Estuary, China. *Remote Sens.* **2017**, *9*, 539. [CrossRef]
- Liu, M.; Mao, D.; Wang, Z.; Li, L.; Man, W.; Jia, M.; Ren, C.; Zhang, Y. Rapid Invasion of *Spartina alterniflora* in the Coastal Zone of Mainland China: New Observations from Landsat OLI Images. *Remote Sens.* **2018**, *10*, 1933. [CrossRef]
- Dong, D.; Wang, C.; Yan, J.; He, Q.; Zeng, J.; Wei, Z. Combining Sentinel-1 and Sentinel-2 image time series for invasive *Spartina alterniflora* mapping on Google Earth Engine: A case study in Zhangjiang Estuary. *J. Applied Remote Sens.* **2020**, *14*, 044504. [CrossRef]
- Zhu, X.; Meng, L.; Zhang, Y.; Weng, Q.; Morris, J. Tidal and Meteorological Influences on the Growth of Invasive *Spartina alterniflora*: Evidence from UAV Remote Sensing. *Remote Sens.* **2019**, *11*, 1208. [CrossRef]
- Xu, R.; Zhao, S.; Ke, Y. A simple phenology-based vegetation index for mapping invasive *Spartina alterniflora* using Google Earth engine. *IEEE J. STARS* **2020**, *14*, 190–201. [CrossRef]
- Tian, J.; Wang, L.; Yin, D.; Li, X.; Diao, C.; Gong, H.; Shi, C.; Menenti, M.; Ge, Y.; Nie, S.; et al. Development of spectral-phenological features for deep learning to understand *Spartina alterniflora* invasion. *Remote Sens. Environ.* **2020**, *242*, 111745. [CrossRef]

21. Li, H.; Mao, D.; Wang, Z.; Huang, X.; Li, L.; Jia, M. Invasion of *Spartina alterniflora* in the coastal zone of mainland China: Control achievements from 2015 to 2020 towards the Sustainable Development Goals. *J. Environ. Manag.* **2022**, *323*, 116242. [[CrossRef](#)]
22. Li, N.; Li, L.; Zhang, Y.; Wu, M. Monitoring of the invasion of *Spartina alterniflora* from 1985 to 2015 in Zhejiang Province, China. *BMC Ecol.* **2020**, *20*, 7. [[CrossRef](#)] [[PubMed](#)]
23. Chen, M.; Ke, Y.; Bai, J.; Li, P.; Lyu, M.; Gong, Z.; Zhou, D. Monitoring early stage invasion of exotic *Spartina alterniflora* using deep-learning super-resolution techniques based on multisource high-resolution satellite imagery: A case study in the Yellow River Delta, China. *Int. J. Appl. Earth Obs.* **2020**, *92*, 102180. [[CrossRef](#)]
24. Chen, W.; Shi, C. Fine-scale mapping of *Spartina alterniflora*-invaded mangrove forests with multi-temporal WorldView-Sentinel-2 data fusion. *Remote Sens. Environ.* **2023**, *295*, 113690. [[CrossRef](#)]
25. Ren, G.; Wang, J.; Wang, A.; Wang, J.; Zhu, Y.; Wu, P.; Ma, Y.; Zhang, J. Monitoring the Invasion of Smooth Cordgrass *Spartina alterniflora* within the Modern Yellow River Delta Using Remote Sensing. *J. Coastal Res.* **2019**, *90*, 135–145. [[CrossRef](#)]
26. Wang, A.; Chen, J.; Jing, C.; Ye, G.; Wu, J.; Huang, Z.; Zhou, C. Monitoring the invasion of *Spartina alterniflora* from 1993 to 2014 with Landsat TM and SPOT 6 satellite data in Yueqing Bay, China. *PLoS ONE* **2015**, *10*, e0135538. [[CrossRef](#)] [[PubMed](#)]
27. Zhou, Y.; Qiu, C.; Li, Y.; Wang, C.; Zhang, Y.; Huang, W.; Li, L.; Liu, H.; Zhang, D. Integrating UAV data to explore the relationship between microtopographic variation and *Spartina alterniflora* expansion during its early invasion. *Ecol. Indic.* **2023**, *154*, 110633. [[CrossRef](#)]
28. Zhou, Z.; Yang, Y.; Chen, B. Estimating *Spartina alterniflora* fractional vegetation cover and aboveground biomass in a coastal wetland using SPOT6 satellite and UAV data. *Aquat. Bot.* **2018**, *144*, 38–45. [[CrossRef](#)]
29. Windle, A.E.; Staver, L.W.; Elmore, A.J.; Scherer, S.; Keller, S.; Malmgren, B.; Silsbe, G.M. Multi-temporal high-resolution marsh vegetation mapping using unoccupied aircraft system remote sensing and machine learning. *Front. Remote Sens.* **2023**, *4*, 1140999. [[CrossRef](#)]
30. Ng, W.-T.; Rima, P.; Einzmann, K.; Immitzer, M.; Atzberger, C.; Eckert, S. Assessing the Potential of Sentinel-2 and Pléiades Data for the Detection of *Prosopis* and *Vachellia* spp. in Kenya. *Remote Sens.* **2017**, *9*, 74. [[CrossRef](#)]
31. Proença, B.; Frappart, F.; Lubac, B.; Marieu, V.; Ygorra, B.; Bombrun, L.; Michalet, R.; Sottolichio, A. Potential of High-Resolution Pléiades Imagery to Monitor Salt Marsh Evolution after *Spartina* Invasion. *Remote Sens.* **2019**, *11*, 968. [[CrossRef](#)]
32. Wang, J.; Lin, Z.; Ma, Y.; Ren, G.; Xu, Z.; Song, X.; Ma, Y.; Wang, A.; Zhao, Y. Distribution and invasion of *Spartina alterniflora* within the Jiaozhou Bay monitored by remote sensing image. *Acta Oceanol. Sin.* **2022**, *41*, 31–40. [[CrossRef](#)]
33. Zhu, W.; Ren, G.; Wang, J.; Wang, J.; Hu, Y.; Lin, Z.; Li, W.; Zhao, Y.; Li, S.; Wang, N. Monitoring the invasive plant *Spartina alterniflora* in Jiangsu coastal wetland using MRCNN and Long-Time Series Landsat Data. *Remote Sens.* **2022**, *14*, 2630. [[CrossRef](#)]
34. Wang, X.; Wang, L.; Tian, J.; Shi, C. Object-based spectral-phenological features for mapping invasive *Spartina alterniflora*. *Int. J. Appl. Earth Obs.* **2021**, *101*, 102349. [[CrossRef](#)]
35. Sun, C.; Li, J.; Liu, Y.; Zhao, S.; Zheng, J.; Zhang, S. Tracking annual changes in the distribution and composition of saltmarsh vegetation on the Jiangsu coast of China using Landsat time series-based phenological parameters. *Remote Sens. Environ.* **2023**, *284*, 113370. [[CrossRef](#)]
36. Zhao, B.; Zhang, M.; Wang, J.; Song, X.; Gui, Y.; Zhang, Y.; Li, W. Multiple Attention Network for *Spartina Alterniflora* Segmentation Using Multi-temporal Remote Sensing Images. *IEEE Trans. Geosci. Remote Sens.* **2023**, *61*, 5402915. [[CrossRef](#)]
37. Zhao, B.; Zhang, M.; Li, W.; Song, X.; Gao, Y.; Zhang, Y.; Wang, J. Intermediate Domain Prototype Contrastive Adaptation for *Spartina Alterniflora* Segmentation Using Multi-temporal Remote Sensing Images. *IEEE Trans. Geosci. Remote Sens.* **2024**, *62*, 5401314. [[CrossRef](#)]
38. Li, X.; Tian, J.; Li, X.; Yu, Y.; Ou, Y.; Zhu, L.; Zhu, X.; Zhou, B.; Gong, H. Annual mapping of *Spartina alterniflora* with deep learning and spectral-phenological features from 2017 to 2021 in the mainland of China. *Int. J. Remote Sens.* **2024**, *45*, 3172–3199. [[CrossRef](#)]
39. Huang, M.; Zhang, Y.; Zhou, Z.; Zhu, X. A dataset of the UAV remote sensing spatial distribution of *Spartina alterniflora* in the Zhangjiang Estuary of Fujian Province from 2013 to 2022. *Science Data Bank* **2023**, *8*. [[CrossRef](#)]
40. Wang, Y.; Mao, Z.; Xin, Z.; Liu, X.; Li, Z.; Dong, Y.; Deng, L. Assessing the Efficacy of Pixel-Level Fusion Techniques for Ultra-High-Resolution Imagery: A Case Study of BJ-3A. *Sensors* **2024**, *24*, 1410. [[CrossRef](#)]
41. Tucker, C.J. Red and photographic infrared linear combinations for monitoring vegetation. *Remote Sens. Environ.* **1979**, *8*, 127–150. [[CrossRef](#)]
42. Drori, R.; Dan, H.; Sprintsin, M.; Sheffer, E. Precipitation-sensitive dynamic threshold: A new and simple method to detect and monitor forest and woody vegetation cover in sub-humid to arid areas. *Remote Sens.* **2020**, *12*, 1231. [[CrossRef](#)]
43. Otsu, N. A threshold selection method from gray-level histograms. *IEEE Trans. Syst. Man Cybern. Syst.* **1979**, *9*, 62–66. [[CrossRef](#)]
44. Jia, M.; Wang, Z.; Mao, D.; Ren, C.; Wang, C.; Wang, Y. Rapid, robust, and automated mapping of tidal flats in China using time series Sentinel-2 images and Google Earth Engine. *Remote Sens. Environ.* **2021**, *255*, 112285. [[CrossRef](#)]
45. Cortes, C.; Vapnik, V. Support-vector networks. *Mach. Learn.* **1995**, *20*, 273–297. [[CrossRef](#)]
46. Mountrakis, G.; Im, J.; Ogole, C. Support vector machines in remote sensing: A review. *ISPRS J. Photogramm.* **2011**, *66*, 247–259. [[CrossRef](#)]
47. Maulik, U.; Chakraborty, D. Remote Sensing Image Classification: A survey of support-vector-machine-based advanced techniques. *IEEE Geosci. Remote Sens. Mag.* **2017**, *5*, 33–52. [[CrossRef](#)]
48. Wang, Y.; Zhu, X.; Wu, B. Automatic detection of individual oil palm trees from UAV images using HOG features and an SVM classifier. *Int. J. Remote Sens.* **2019**, *40*, 7356–7370. [[CrossRef](#)]

49. Schmidt, K.; Skidmore, A. Spectral discrimination of vegetation types in a coastal wetland. *Remote Sens. Environ.* **2003**, *85*, 92–108. [[CrossRef](#)]
50. Adam, E.; Mutanga, O. Spectral discrimination of papyrus vegetation (*Cyperus papyrus* L.) in swamp wetlands using field spectrometry. *ISPRS J. Photogramm.* **2009**, *64*, 612–620. [[CrossRef](#)]
51. Silvestri, S.; Defina, A.; Marani, M. Tidal regime, salinity and salt marsh plant zonation. *Estuar. Coast. Shelf S.* **2005**, *62*, 119–130. [[CrossRef](#)]
52. Peng, D.; Chen, L.; Pennings, S.C.; Zhang, Y. Using a marsh organ to predict future plant communities in a Chinese estuary invaded by an exotic grass and mangrove. *Limnol. Oceanogr.* **2018**, *63*, 2595–2605. [[CrossRef](#)]
53. Xu, H. Modification of normalised difference water index (NDWI) to enhance open water features in remotely sensed imagery. *Int. J. Remote Sens.* **2006**, *27*, 3025–3033. [[CrossRef](#)]
54. Huete, A.; Liu, H.; Batchily, K.; Van Leeuwen, W. A comparison of vegetation indices over a global set of TM images for EOS-MODIS. *Remote Sens. Environ.* **1997**, *59*, 440–451. [[CrossRef](#)]
55. Xiao, X.; Boles, S.; Liu, J.; Zhuang, D.; Liu, M. Characterization of forest types in Northeastern China, using multi-temporal SPOT-4 VEGETATION sensor data. *Remote Sens. Environ.* **2002**, *82*, 335–348. [[CrossRef](#)]
56. Shi, T.; Liu, J.; Hu, Z.; Liu, H.; Wang, J.; Wu, G. New spectral metrics for mangrove forest identification. *Remote Sens. Lett.* **2016**, *7*, 885–894. [[CrossRef](#)]
57. Fundisi, E.; Tesfamichael, S.G.; Ahmed, F. A combination of Sentinel-1 RADAR and Sentinel-2 multispectral data improves classification of morphologically similar savanna woody plants. *Eur. J. Remote Sens.* **2022**, *55*, 372–387. [[CrossRef](#)]
58. Blickensdörfer, L.; Schwieder, M.; Pflugmacher, D.; Nendel, C.; Erasmi, S.; Hostert, P. Mapping of crop types and crop sequences with combined time series of Sentinel-1, Sentinel-2 and Landsat 8 data for Germany. *Remote Sens. Environ.* **2022**, *269*, 112831. [[CrossRef](#)]
59. Ienco, D.; Interdonato, R.; Gaetano, R.; Minh, D.H.T. Combining Sentinel-1 and Sentinel-2 Satellite Image Time Series for land cover mapping via a multi-source deep learning architecture. *ISPRS J. Photogramm.* **2019**, *158*, 11–22. [[CrossRef](#)]
60. Wilson, K.L.; Wong, M.C.; Devred, E. Comparing Sentinel-2 and WorldView-3 imagery for coastal bottom habitat mapping in Atlantic Canada. *Remote Sens.* **2022**, *14*, 1254. [[CrossRef](#)]
61. Kovacs, E.; Roelfsema, C.; Lyons, M.; Zhao, S.; Phinn, S. Seagrass habitat mapping: How do Landsat 8 OLI, Sentinel-2, ZY-3A, and Worldview-3 perform? *Remote Sens. Lett.* **2018**, *9*, 686–695. [[CrossRef](#)]
62. Marcello, J.; Eugenio, F.; Gonzalo-Martin, C.; Rodriguez-Esparragon, D.; Marques, F. Advanced processing of multiplatform remote sensing imagery for the monitoring of coastal and mountain ecosystems. *IEEE Access* **2020**, *9*, 6536–6549. [[CrossRef](#)]
63. Dattola, L.; Rende, S.F.; Dominici, R.; Lanera, P.; Di Mento, R.; Scalise, S.; Cappa, P.; Oranges, T.; Aramini, G. Comparison of Sentinel-2 and Landsat-8 OLI satellite images vs. high spatial resolution images (MIVIS and WorldView-2) for mapping *Posidonia oceanica* meadows. In Proceedings of the Remote Sensing of the Ocean, Sea Ice, Coastal Waters, and Large Water Regions 2018, Berlin, Germany, 10–12 September 2018; pp. 252–262.
64. Xiao, Y.; Tang, J.; Qing, H.; Zhou, C.; Kong, W.; An, S. Trade-offs among growth, clonal, and sexual reproduction in an invasive plant *Spartina alterniflora* responding to inundation and clonal integration. *Hydrobiologia* **2011**, *658*, 353–363. [[CrossRef](#)]
65. Liu, H.; Lin, Z.; Qi, X.; Zhang, M.; Yang, H. The relative importance of sexual and asexual reproduction in the spread of *Spartina alterniflora* using a spatially explicit individual-based model. *Ecol. Res.* **2014**, *29*, 905–915. [[CrossRef](#)]
66. Daehler, C.C.; Strong, D.R. Variable reproductive output among clones of *Spartina alterniflora* (Poaceae) invading San Francisco Bay, California: The influence of herbivory, pollination, and establishment site. *Am. J. Botany* **1994**, *81*, 307–313. [[CrossRef](#)]
67. Vitousek, P.M.; d’Antonio, C.M.; Loope, L.L.; Westbrooks, R. Biological invasions as global environmental change. *Am. Sci.* **1996**, *84*, 468–478.
68. Nie, M.; Liu, W.; Pennings, S.C.; Li, B. Lessons from the invasion of *Spartina alterniflora* in coastal China. *Ecology* **2023**, *104*, e3874. [[CrossRef](#)] [[PubMed](#)]
69. Strong, D.R.; Ayres, D.R. Ecological and evolutionary misadventures of *Spartina*. *Annu. Rev. Ecol. Evol. Syst.* **2013**, *44*, 389–410. [[CrossRef](#)]
70. Zheng, X.; Javed, Z.; Liu, B.; Zhong, S.; Cheng, Z.; Rehman, A.; Du, D.; Li, J. Impact of *Spartina alterniflora* invasion in coastal wetlands of China: Boon or bane? *Biology* **2023**, *12*, 1057. [[CrossRef](#)]
71. Zheng, J.; Wei, H.; Chen, R.; Liu, J.; Wang, L.; Gu, W. Invasive trends of *Spartina alterniflora* in the southeastern Coast of China and potential distributional impacts on mangrove forests. *Plants* **2023**, *12*, 1923. [[CrossRef](#)]
72. Zhao, Z.; Yuan, L.; Li, W.; Tian, B.; Zhang, L. Re-invasion of *Spartina alterniflora* in restored saltmarshes: Seed arrival, retention, germination, and establishment. *J. Environ. Manag.* **2020**, *266*, 110631. [[CrossRef](#)] [[PubMed](#)]

**Disclaimer/Publisher’s Note:** The statements, opinions and data contained in all publications are solely those of the individual author(s) and contributor(s) and not of MDPI and/or the editor(s). MDPI and/or the editor(s) disclaim responsibility for any injury to people or property resulting from any ideas, methods, instructions or products referred to in the content.